LAWRENCE
LIVERMORE
NATIONAL
LABORATORY

LLNL-JRNL-421074

Symmetry tuning via controlled crossed-beam energy transfer on the National Ignition Facility

P. Michel, S. H. Glenzer, L. Divol, D. Callahan, S. Dixit, D. Hinkel, R. K. Kirkwood, W. L. Kruer, G. A. Kyrala, N. B . Meezan, R. Town, E. A. Williams, B. J. MacGowan, J. Lindl, L. J. Suter

December 7, 2009

Plasma of Physics

Disclaimer

Symmetry tuning via controlled crossed-beam energy transfer on the National Ignition Facility

P. Michel, S. H. Glenzer, L. Divol, D. Callahan, S. Dixit, D. Hinkel, R. K. Kirkwood, W. L. Kruer, G. A. Kyrala, N. B. Meezan, R. Town, E. A. Williams, B. J. MacGowan, J. Lindl, and L. J. Suter
Lawrence Livermore National Laboratory, Livermore, CA 94551

The hohlraum energetics experimental campaign started in the summer of 2009 on the national Ignition Facility (NIF) (cf. N. Meezan et al., Phys. Plasmas, this issue). These experiments have demonstrated controlled crossed-beam transfer as an efficient and robust tool to tune the implosion symmetry of ignition capsules. A new linear model calculating crossed-beam energy transfer between cones of beams on the NIF has been developed. The model has been applied to the emulator targets shot for the National Ignition Campaign in 2009. These targets have no lip liner at the laser entrance holes, which reduces the amount of energy transfer between laser beams and requires a larger wavelength separation between the cones of laser beams in order to achieve the best symmetry (with no net transfer between the inner and outer cones). A good agreement is found between the calculations and measurements; remaining discrepancies can be explained by a 10% error in modeling the flow at the laser entrance hole of ignitions hohlraums.

I. INTRODUCTION

Energy transfer between laser beams crossing in a plasma has been extensively studied over the last decade due to its possible impact on ignition experiments on facilities such as the National Ignition Facility (NIF) [1, 2]. In these experiments, two crossing laser beams can transfer energy to one another via stimulated Brillouin scattering (SBS), i.e. a three waves process between the two beams and the ion acoustic wave (IAW) excited by their beat wave (cf. Refs. [3, 4] and references therein). The relevance of this process for ignition experiments was first pointed out by Kruer et al. [5]. It was noted that a "four-color" laser smoothing scheme considered back then could lead to resonant interaction between laser beams crossing at the laser entrance holes (LEH) of hohlraum targets, which could in turn affect the implosion symmetry. This paper also emphasized the importance of the variations in frequency separation between the beams for understanding and controlling the interactions between crossing laser beams. Soon after, Kirkwood et al. started a series of experiments that demonstrated energy transfer between laser beams and its dependence to a frequency separation between the laser beams [6, 7]; later work established the sensivity of crossed-beam transfer to plasma flow for two laser beams of same wavelength [8, 9] and its saturation due to plasma waves non-linearities [10]. Significant numerical and theoretical work has been achieved by several groups on the topic [11–13], with a focus on plasma waves non-linearities in order to model the experiments that showed strong non-linear saturation of the transfer process with energy gains much smaller than linear predictions.

It was only in 2003 and 2004 that Williams et al. [14, 15] established that the IAW associated with the crossed-beam transfer process would actually be linear ($\delta n/n \ll 1$) in the conditions of ignition experiments on the NIF, and that no trapping or non-linear saturation process should be expected. The first quantitative estimates of energy transfer between laser beams in a NIF hohlraum were provided using ray tracing between a few pairs of beams. It was also shown that a wavelength separation between cones of beams should allow a control of the energy transfer. A "two-color" option was then implemented on NIF; this scheme allows to change the wavelength of the "outer beams" (hitting the hohlraum walls near the laser entrance holes (LEH) in order to provide x-ray flux on the poles of the capsule) with respect to the wavelength of the "inner beams" (that hit the waist of the hohlraum in order to provide x-ray flux on the equator of the capsule). The goal of that option was to compensate for crossed-beam energy transfer is necessary.

This ultimately led to a deeper and more comprehensive assessment of the crossed-beam transfer process in NIF hohlraums [16, 17], where a three-dimensional steady-state model was used to investigate the process in NIF conditions, including the effects of laser beams smoothing. Quantitative calculations of energy transfer between cones of laser beams were made, and the effect on implosion symmetry was calculated by coupling the crossed-beam transfer model to view-factor of hydrodynamics codes. It was then claimed that the process could be controlled and actually used as a *tool* to tune the implosion symmetry and compensate for possible impaired propagation of some of the laser beams due to other laser-plasma instabilities (LPI) occurring deeper in the hohlraum.

In this paper, we will present the results of the first cryogenic targets experiments on NIF, which demonstrated the efficiency of crossed-beam transfer as a tool to tune the implosion symmetry. We will present a new model that was used to make faster assessments of crossed-beam transfer on various target designs, including the emulator hohlraums shot in the early phase of the Hohlraum Energetics Campaign on NIF. The targets used for these experiments did not have a plastic lip liner at the LEH anymore; we will explain the impact of re-

moving the LEH liner for crossed-beam energy transfer and show predictions for these two types of targets. We will then compare the predictions to the experimental measurements.

II. MULTI-BEAMS LINEAR MODEL FOR RAPID CROSSED-BEAM TRANSFER ASSESSMENTS

We have developed a new numerical tool for rapid assessment of crossed-beam energy transfer in NIF hohlraum designs. Like the model described in Refs. [16, 17], this model is steady-state and calculates energy transfer on 3D hydrodynamic profiles from Lasnex [18] or Hydra [19] simulations. The IAW response is also based on a linear kinetic model similar to Refs. [14, 20]. Several changes have been made compared to [16, 17]:

- we neglect any refraction of the laser beams, based on the fact that the beams undergo very less of it at the LEH where the electron density is low;
- we neglect diffraction, due to the large spot sizes and interaction lengths smaller than the Rayleigh length of the beams;
- we neglect the speckles structure of the beams; we had already established that the convective gain for energy transfer between two beams is small in NIF conditions ($g \ll 1$), over typical interaction lengths of 1-2 mm. Therefore, the gain is also $\ll 1$ over a speckle length ($\approx 100\ \mu$m), even in the most intense speckles.

Neglecting these three aspects is equivalent to neglecting the 3D nature of the laser beams. On the other hand, this removes the constraints of the paraxial approximation that limited our previous model to calculating energy transfer between pairs of beams only, with subsequent linear estimates of the transfer of each beam to each of its nearest neighbors [16, 17].

Our new model solves a set of 24 equations, one for each of the 24 quads of laser beams going through the LEH of a hohlraum. Each equation calculates the envelope of the electric field a_{0j} (for j=1 to 24), and has the following form:

$$(\partial_z + \nu)\, a_{0j} = -\frac{i}{2} \sum_{q=1}^{24} \frac{|\boldsymbol{k}_{0q} - \boldsymbol{k}_{0j}|^2}{8 k_{0j}} \frac{\chi_e (1+\chi_i)}{\epsilon} |a_{0q}|^2 a_{0j}, \quad (1)$$

where ν stands for the inverse Bremsstrahlung absorption, $\boldsymbol{k}_{0q}$ is the wave vector of the quad q, χ_e, χ_i are the electron and ion susceptibilities and $\epsilon = 1 + \chi_e + \chi_i$ is the dielectric constant. The factor $\frac{1}{2}$ accounts for the polarization smoothing effect (cf. Ref. [17]). SSD can also be accounted for in a similar manner as in Ref. [17], however it should have a negligible effect in the new target designs without LEH liners due to much broader resonances (larger than the SSD bandwidth) - cf. next section.

We thus calculate the coupling of all the beams altogether; each beam is coupled to all the other beams with full pump depletion. We model each quadruplet ("quad") of beams without distinguishing the individual beams within. The intensity profiles are assumed uniform, with dimensions and power specified by the phase plates and laser pulse shapes used for each given target design. Fig. 1 represents the 24 quads overlapping near the LEH of a NIF hohlraum, without crossed-beam transfer.

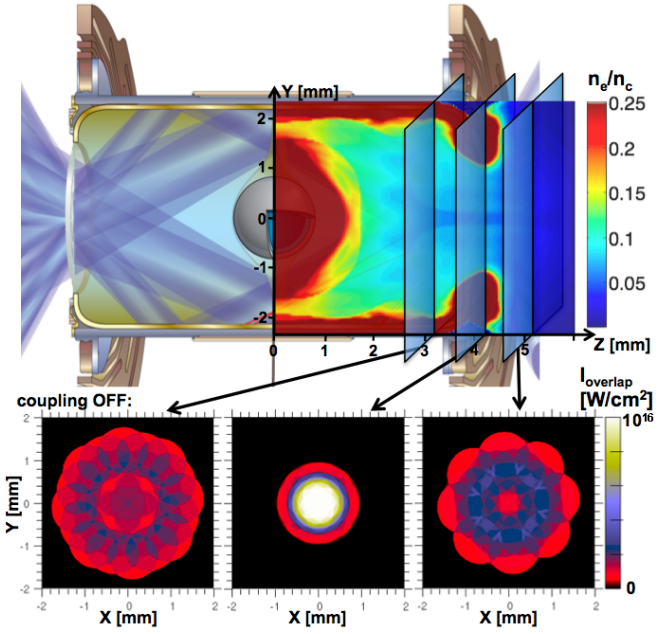

FIG. 1: (Color online) Top: NIF hohlraum, with electron density profile from a Lasnex simulation. Bottom: intensity of the 24 incoming laser quads in the transverse (X,Y) plane, at the three indicated Z-positions (Z=3.2, 4.2 and 5.2 mm; 4.2 mm is the LEH position). The intensity is defined with the Poynting vector in the Z-direction.

This model allows a very fast assessment of crossed-beam transfer between cones of beams on different NIF target designs. Because it is computationally efficient, the model is also run at several time across the laser pulse. Note that it is not coupled to the hydrodynamics codes in a consistent manner yet, but this is currently under development.

III. APPLICATION OF THE CROSSED-BEAM MODEL TO RECENT NIF EMULATOR TARGETS

The first series of experiments on the NIF in 2009 relied on an "emulator" target, which goal is to provide internal

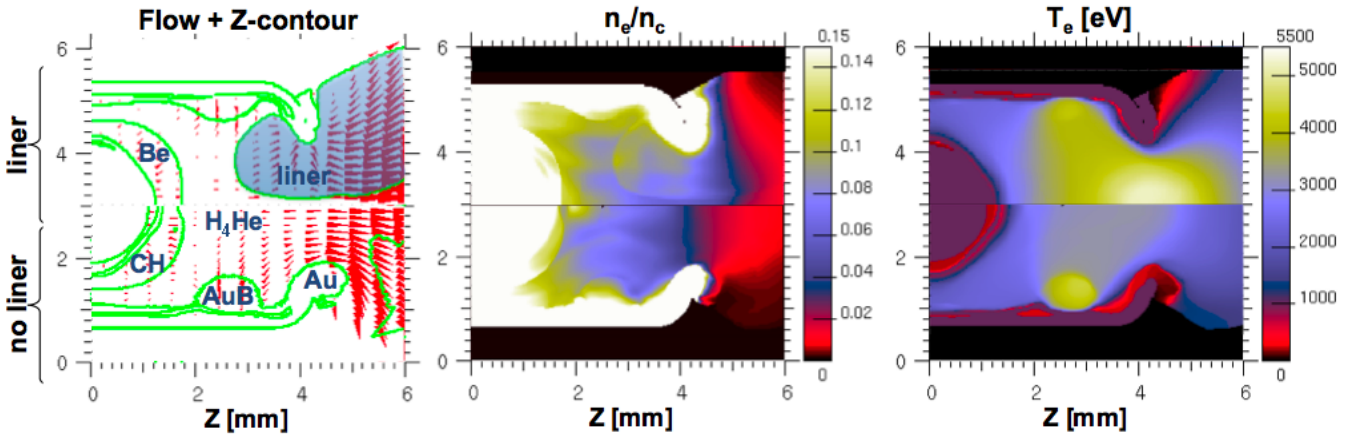

FIG. 2: (Color online) Hydrodynamic profiles for an emulator hohlraum with (top halves) and without (bottom halves) an LEH liner. The Z contours show the frontiers between the gas (H_4He in both cases), the LEH liner material (CH), the ablator (Be or CH), the gold hohlraum wall and its Au-B liner (designed to reduce to amount of SBS from the outer beams). The hydrodynamics profiles for the lined LEH hohlraum are from Lasnex simualtions, while the unlined are from Hydra; both are taken at the time of peak laser power.

hohlraum conditions similar to full scale targets but with less laser energy ($\simeq$ 500 to 700 kJ instead of 1.2 to 1.5 MJ) [21]. The emulator hohlraums are typically subscaled by about 20%. The target design underwent some significant changes before the experiments; perhaps the most noticeable change is the suppression of the LEH lip liner. This was motivated by the recently-investigated risk of amplification of the backscatter light generated inside the hohlraum as it interacts with all the incoming laser beams at the LEH [22].

Besides reducing the gains for multi-beams amplification of backscatter, removing the LEH liners also reduces the gains for crossed-beam energy transfer. Fig. 2 shows the hydrodynamic profiles for hohlraum emulators. The Brillouin gains are reduced due to a lower Zn_e/T_e ratio; indeed, the beams cross in the H_4He gas instead of the CH plasma from the liner, and both the density and temperature are significantly reduced ($n_e/n_c \approx 2\%$ instead of 6-7% with a liner, and $T_e \approx 3$ keV vs. 5-6 keV with a liner). Note that the flow structure is also different. The LEH liner creates a flow going towards the inside of the hohlraum in the vicinity of the LEH, while removing it leads to an exclusively outwards flow.

Fig. 3-a shows the energy transfer as calculated by our model for a 0.78x scale hohlraum emulator with and without an LEH liner. The "inner cone" and "outer cone" curves correspond to the average energy transfer over all the inner and outer beams, respectively. For a given $\Delta\lambda$, the outer cone transfer is half the inner's, because there is about twice more energy in the outer cone than in the inner. The two curves cross for a wavelength separation of 0.1 Å (lined LEH target) and 1.5 Å (unlined LEH target). The crossing point corresponds to a zero net average transfer between the inner and outer cones (yet there is still residual transfer between some of the beams, as explained in ref. [17]).

With a liner, the slopes of the curves of transfer vs. $\Delta\lambda$ are significantly steeper than without a liner, even reaching depletion of the cones (as the inner cone has roughly half the energy of the outer cone, it can triple its own energy as it fully pumps out the outer beams, i.e. a relative gain of +200%). $\Delta\lambda$ on these plots is the wavelength shift between the inner and outer cones as explained in Ref. [16] (the outer cone wavelength is blue-shifted by $\Delta\lambda$ with respect to the inner cone wavelength), and is defined at the fundamental frequency of the laser (1ω), before frequency conversion to the third harmonic.

Another noticeable difference between the two targets is that the $\Delta\lambda$ of optimum symmetry (i.e. zero net transfer between the inner and outer cones) is shifted towards a longer wavelength separation, 1.5 Å instead of 0.1 Å. This is explained by the difference in the flow structure near the LEH. As noticed and explained in Ref. [17], for $\Delta\lambda = 0$ the inwards flow introduced by the expanding LEH creates a zone slightly inside the hohlraum where there is energy transfer from the outer to the inner beams; this compensates for the outwards flow just outside the hohlraum that leads to transfer to the outer beams. Without an LEH liner, the flow near the LEH goes only outwards: thus, there is more transfer from the inner to the outer beams at $\Delta\lambda = 0$, requiring more wavelength separation to cancel the net transfer between the inner and outer cones.

Fig. 3-b represents the calculated laser beams profiles on the hohlraum walls for $\Delta\lambda$=0, 1.5 and 3 Å. This clearly shows the energy transfer going from the outer to the inner beams as we increase $\Delta\lambda$, as well as the modification of the intensity profiles as was already described in Ref. [17].

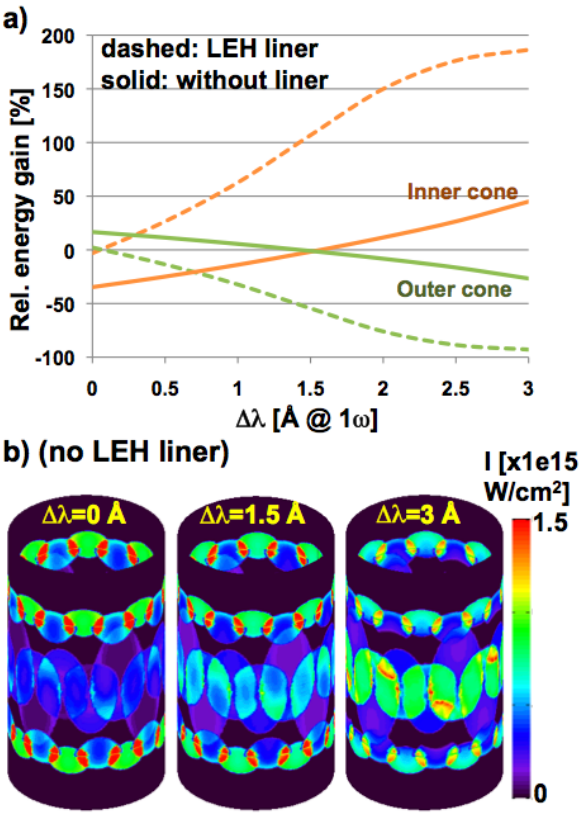

FIG. 3: (Color online) a) Relative energy gain from crossed-beam transfer averaged over the inner cones and the outer cones, for the hohlraum emulator with (dashed) and without (solid) an LEH liner. b) Intensity profiles for all the beams as they reach the hohlraum walls, for a wavelength separation of 0, 1.5 Å and 3 Å between the inner and outer cones (with $\lambda_{outer} = \lambda_{inner} - \Delta\lambda$). This is for a hohlraum without LEH liner ($\Delta\lambda$=1.5Å is the point of best symmetry).

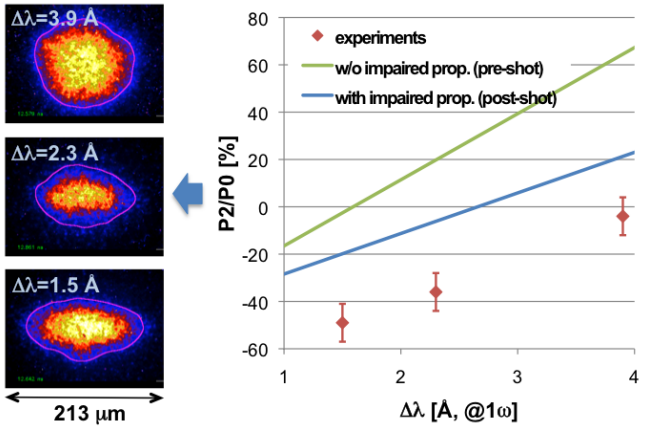

FIG. 4: (Color online) Left: GXD images of the capsule for three wavelength separation between the inner and outer beams: 1.5, 2.3 and 3.9 Å. Right: P2/P0 (pole-waist asymmetry) for the corresponding three shots

IV. EXPERIMENTAL RESULTS AND COMPARISON WITH PREDICTIONS

The first cryogenic hohlraums were shot on NIF as part of the hohlraum energetics campaign in September 2009 (cf. Ref. [21]). These were filled with a gas mixture of H_4He, and had no LEH liner. The laser pulse length was 11 ns, with a peak power of about 4 TW per quad delivering a total of 0.5 MJ of 3ω light on target.

The implosion symmetry is measured using the gated x-ray diagnostic (GXD), which takes a series of snapshots of the capsule x-ray self-emission at different times around "bang time" (i.e. time of peak x-ray emission). The snapshots are integrated over about 200 ps, and the images are collected through an x-ray pinhole mounted in front of multi-chanel plate CCD. The hohlraums feature a small plastic window on the waist that allows to take these capsule images.

To quantify the implosion symmetry, we decompose the x-ray flux iso-contours from the GXD images onto spherical harmonics. The ratio P_2/P_0 of the coefficients of $Y_2^0(\theta)$ and Y_0^0 for the 18% x-ray flux contour provides a measure of the pole-waist asymmetry ($P_2 < 0$ corresponds to an oblate or "pancake" implosion, i.e. with too much compression on the poles of the capsule, while $P_2 > 0$ corresponds to a prolate or "sausage" implosion, i.e. with too much compression on the equator of the capsule).

Fig. 4 shows the experimental results from the first cryogenic shots on NIF. On the left side of the image are three GXD images at bang time for three wavelength separations of 1.5, 2.3 and 3.9 Å. The first shot was setup with a separation of 1.5 Å, for which we expected best symmetry according to our calculations. However, a significant amount of stimulated Raman scattering (SRS) was measured on the inner beams for this shot; the measured reflectivity for the quadruplet on which the backscatter was measured (at 30° from axis) was 19% time-integrated (i.e. about 6% total reflectivity, since a third of the total energy goes into the inner beams). Negligible backscatter was measured on the outer beams (less than 1% total). This means that the inner beams propagation was significantly impaired (note that we cannot measure the SRS that gets reabsorbed inside the hohlraum, which adds to the impairment). This corresponds to a lack of x-ray drive on the waist of the capsule, which in turns leads to an oblate implosion. The P_2/P_0 ratio for this shot was -49%.

Note that new target designs with a pure He gas fill have since then been used, and have shown a reduction of SRS by about a factor two (SRS reflectivities do not exceed 10% anymore).

As we increased $\Delta\lambda$ to 2.3 Å and then 3.9 Å on the next shots, the asymmetry went from -49% to -36% and ultimately -4%, reaching a nearly round implosion. Note that the outer beams wavelength was the only param-

eter that was changed; we did not modify the beams energy or cone fraction during these shots. This result unambiguously validates the two-color separation as an efficient and robust was to tune the implosion symmetry of ignition targets, as was previously predicted in Ref. [16].

An important observation made during these shots was that the amount of SRS on the inner beams did not change, and stayed at 19% reflectivity. This is still under investigation, and will be the object of future publications. On the other hand, the outer beams backscatter went down dramatically as we increased $\Delta\lambda$, from about 1% total to less than 0.01%. However this is energetically negligible and should not affect the symmetry either.

Fig. 4 also shows the comparison between the experimental data and the calculations. The calculations were run using the following approach:

First, hydrodynamic simulations were done before the shots. These obviously did not account for any backscatter and used the "requested" laser pulse shape and energy. The crossed-beam transfer model was then run at several times around peak laser power on these hydrodynamic profiles, and the energy transfer was calculated for each beam *a posteriori*, i.e. in a non-consistent way. The new laser pulse shapes for each individual beam that included crossed-beam energy transfer were then used to run a second series of calculations, from which we extracted the implosion symmetry measurement shown as the green curve on Fig. 4 ("pre-shot, without impaired propagation"). The curve predicts a best symmetry at $\Delta\lambda$=1.5 Å, and is also steeper than the experimental measurements.

Then, after the shots, a second analysis was run. This included the impaired propagation of the laser beams due to SRS (this is modeled by changing the laser wavelength of the rays in the hydrodynamic simulations in order to increase the absorption before the rays reach the hohlraum walls; this mocks-up the impaired propagation due to SRS). This also included the *measured* (i.e. as-shot, as opposed to as-requested) laser pulse shapes. The results from this analysis correspond to the blue curve on Fig. 4 ("post-shot, with impaired propagation").

Accounting for the impairment in the inner beams propagation brings the calculations in closer agreement to the experiments. The slope of the curve of P_2/P_0 is similar to the experiments, however there is still a shift in the wavelength separation of optimum symmetry, of about 1.5 Å.

Fig. 5 shows the curves of transfer vs. $\Delta\lambda$ over a more relevant range, which is the range that resolves the ion acoustic velocity near the LEH. The curves saturate near +200%/-100% for the inner cone and +50%/-100% for the outer cone (due to the cone fraction of about 1/3), due to depletion of the laser. Note that other saturation mechanisms not accounted for in our model might come into play for such large transfer values.

The separation between the two resonances corresponds to twice the ion acoustic velocity multiplied by

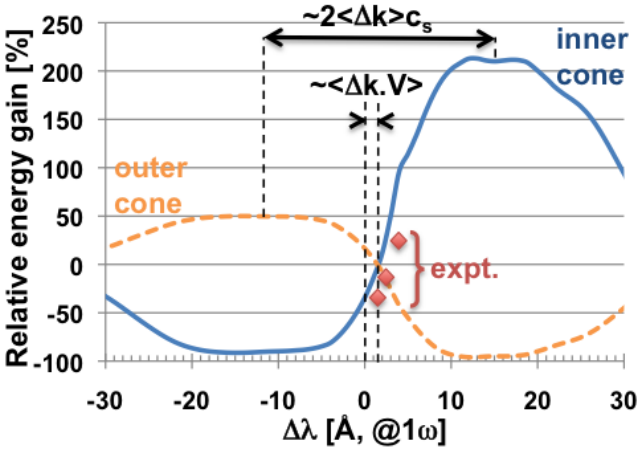

FIG. 5: (Color online) blablabla.

an average $< \boldsymbol{\Delta k} >$ (which can be seen as an average difference between the wave vector of the outer beams and that of the inner beams). The curves do not cross at $\Delta\lambda$=0 due to the flow structure at the LEH; the crossing point corresponds to an average (over all the possible pairs of beams) of $< \boldsymbol{\Delta k} \cdot \boldsymbol{V} >$ where $\boldsymbol{V}$ is the average flow at the LEH. The three red points correspond to the inner cone transfer from the experiments and are shifted by 1.5 Å. This basically shows that only a 10% error in the modeling of the flow at the LEH can be responsible for the observed shift in optimum $\Delta\lambda$. This also shows that the experiments and calculations are in very good agreement once plotted on a relevant range of $\Delta\lambda$.

As a final remark, note that the two-color method for symmetry tuning has been repeated on different targets (in particular on hohlraums with pure He gas-fill, which produce about 10% SRS on the inner beams - i.e. about 3% of the total energy, as only a third of the total laser energy goes into the inner beams). The results have been very robust and repeatable. A more comprehensive analysis of crossed-beam transfer in the experiments vs. calculations is still under way, and will be the topic of a separate, longer publication.

V. CONCLUSION

In summary, we have demonstrated that controlling the crossed-beam energy transfer by shifting the wavelengths of some of the beams was a reliable and efficient way to tune the implosion symmetry in ignition experiments. This method allows to compensate for impaired propagation of some of the beams due to backscatter instabilities inside the hohlraum such as stimulated Raman or Brillouin scattering. In the early NIF experiments in September 2009, this allowed to recover a round implosion after starting from a very oblate one with significant SRS on the inner beams. The amounts of energy transfer

obtained are very large (about 50% or more), and allow us to tune the effective cone fraction without changing the laser energy at all. This technique has proven to be an invaluable tool in the NIF experimental campaign.

Calculations were performed using a new numerical model, that provides rapid assessments of new target designs and post-shot analysis. The calculations are in good agreement with the measurements; the remaining differences can be explained by both the impaired propagation of the laser beams and some error in modeling the detailed structure of the flow at the LEH of the hohlraums.

Acknowledgments

The authors gratefully acknowledge the efforts and dedication of the NIF team for the experiments and their preparation. This work was performed under the auspices of the U.S. Department of Energy by Lawrence Livermore National Laboratory under Contract DE-AC52-07NA27344.

[1] J. D. Lindl, P. Amendt, R. L. Berger, S. G. Glendinning, S. H. Glenzer, S. W. Haan, R. L. Kauffman, O. L. Landen, and L. J. Suter, Phys. Plasmas **11**, 339 (2004).
[2] E. I. Moses, R. N. Boyd, B. A. Remington, C. J. Keane, and R. Al-Ayat, Physics of Plasmas **16**, 041006 (2009).
[3] L. M. Gorbunov, Soviet Physics JETP **28**, 1220 (1969).
[4] W. L. Kruer, *The physics of laser plasma interactions* (Westview Press, 2003).
[5] W. L. Kruer, S. C. Wilks, B. B. Afeyan, and R. K. Kirkwood, Phys. Plasmas **3**, 382 (1996).
[6] R. K. Kirkwood, B. B. Afeyan, W. L. Kruer, B. J. MacGowan, J. D. Moody, D. S. Montgomery, D. M. Pennington, T. L. Weiland, and S. C. Wilks, Phys. Rev. Lett. **76**, 2065 (1996).
[7] R. K. Kirkwood, B. J. MacGowan, D. S. Montgomery, B. B. Afeyan, W. L. Kruer, D. M. Pennington, S. C. Wilks, J. D. Moody, K. Wharton, C. A. Back, et al., Phys. Plasmas **4**, 1800 (1997).
[8] K. B. Wharton, R. K. Kirkwood, S. H. Glenzer, K. G. Estabrook, B. B. Afeyan, B. I. Cohen, J. D. Moody, and C. Joshi, Phys. Rev. Lett. **81**, 2248 (1998).
[9] K. B. Wharton, R. K. Kirkwood, S. H. Glenzer, K. G. Estabrook, B. B. Afeyan, B. I. Cohen, J. D. Moody, B. J. MacGowan, and C. Joshi, Phys. Plasmas **6**, 2144 (1999).
[10] R. K. Kirkwood, J. D. Moody, A. B. Langdon, B. I. Cohen, E. A. Williams, M. R. Dorr, J. A. Hittinger, R. Berger, P. E. Young, L. J. Suter, et al., Phys. Rev. Lett. **89**, 215003 (2002).
[11] V. V. Eliseev, W. Rozmus, V. T. Tikhonchuk, and C. E. Capjack, Phys. Plasmas **6**, 3 (1996).
[12] C. J. McKinstrie, J. S. Liu, R. E. Giacone, and H. X. Vu, Phys. Plasmas **7**, 3 (1996).
[13] J. Hittinger, M. Dorr, R. Berger, and E. Williams, Journal of Computational Physics **209**, 695 (2005), ISSN 0021-9991.
[14] E. A. Williams, B. I. Cohen, L. Divol, M. R. Dorr, J. A. Hittinger, D. E. Hinkel, A. B. Langdon, R. K. Kirkwood, D. H. Froula, and S. H. Glenzer, Phys. Plasmas **11**, 231 (2004).
[15] E. A. Williams, D. E. Hinkel, and J. A. Hittinger, in *Inertial Fusion Sciences and Applications 2003* (The American Nuclear Society, 2004), p. 252.
[16] P. Michel, L. Divol, E. A. Williams, S. Weber, C. A. Thomas, D. A. Callahan, S. W. Haan, J. D. Salmonson, S. Dixit, D. E. Hinkel, et al., Phys. Rev. Lett. **102**, 025004 (2009).
[17] P. Michel, L. Divol, E. A. Williams, C. A. Thomas, D. A. Callahan, S. Weber, S. W. Haan, J. D. Salmonson, N. B. Meezan, O. L. Landen, et al., Physics of Plasmas **16**, 042702 (pages 9) (2009).
[18] G. B. Zimmerman and W. L. Kruer, Comments Plasma Phys. Control. Fusion **2**, 51 (1975).
[19] M. M. Marinak, G. D. Kerbel, N. A. Gentile, O. Jones, D. Munro, S. Pollaine, T. R. Dittrich, and S. W. Haan, Physics of Plasmas **8**, 2275 (2001).
[20] J. F. Drake, P. K. Kaw, Y. C. Lee, G. Schmidt, C. S. Liu, and M. N. Rosenbluth, Phys. Fluids **17**, 778 (1974).
[21] N. B. Meezan, L. J. Atherton, D. A. Callahan, E. L. Dewald, S. Dixit, E. G. Dzenitis, M. J. Edwards, C. A. Haynam, D. E. Hinkel, O. S. Jones, et al., Physics of Plasmas (2010), this issue.
[22] P. Michel et al. (2010), in preparation.